RESEARCH REPORT

VTT-R-00899-10

Flaw detection trials using virtual ultrasonic testing

Authors: Matti Sarkimo

Confidentiality: Public

Report's title

Flaw detection trials using virtual ultrasonic testing

Customer, contact person, address	Order reference
SAFIR 2010, VYR	
Project name	**Project number/Short name**
Risk-Informed Inspections of Piping / SAFIR2010	32525/PURISTA
Author(s)	**Pages**
Matti Sarkimo	18/3
Keywords	**Report identification code**
NDT, non-destructive testing, ultrasonic inspection, modeling, simulation	VTT-R-00899-10

Summary

This report discusses first some general features which should be considered when Civa ultrasonic simulation program is applied in virtual inspection trials. Then a simulation trial implementation and results are reported. The main purpose of this study was to test different features of Civa in creation and analysis of a virtual detectablity trial.

A series of simulations was computed using simple plate formed test block that included notch shaped flaws with varying depths. To make the case realistic and meaningful in the analysis phase significant structural noise and moderate attenuation were added to the simulation using the material properties settings. The simulation was run using with different probe frequency values and crystal dimensions to produce variation in the flaw detectablity.

The simulation data files resembling ultrasonic inspection data files were analyzed using Civa analysis tools. The signal-to-noise ratios and locations of the detected indication were measured. Finally an assessment was made concerning detectablity dependence on the notch height. Also some study about signal-to-noise ratios measured from the detected indications was performed.

Confidentiality	Public

Espoo 28.1.2010

Written by	Reviewed by	Accepted by
Matti Sarkimo, Senior Research Scientist	Esa Leskelä, Research Scientist	Pentti Kauppinen, Technology Manager

VTT's contact address

VTT Technical Research Centre of Finland, P.O. Box 1000, FI-02044 VTT, Finland

Distribution (customer and VTT)

SAFIR 2010 / PURISTA distribution

Preface

This report has been prepared in the research project Risk-Informed Inspections of Piping. This project is a part of the SAFIR2010, the Finnish Research Program on Nuclear Power Plant Safety for years 2007 – 2010. The work was carried out at VTT, Technical Research Centre of Finland. The work has been funded by the State Nuclear Waste Management Fund (VYR) and VTT.

Espoo 28.1.2010

Authors

Contents

1 Introduction

When ultrasonic inspection technique is developed for a specific component there is often a need for practical trials. One wants to test the performance of the inspection system and the available parameter choices to achieve the best outcome. In the qualification process there are often also official requirements for practical test trials.

The production of the real test blocks is usually expensive and time consuming. Also the number of the defects that can be introduced in the test block is often quite limited. Ultrasonic inspection simulations using computers offer a possibility to create virtual test blocks that can be applied to imitate practical trials. The component and flaw properties (e.g. material, geometry, noise level, defect size, defect location and defect orientation) or inspection parameters (e.g. inspection technique, and probe characteristics) can be varied very flexibly and quickly.

Inspection of a virtual test block means running simulation using similar scan pattern as the real inspection. The simulation computation can take from minutes to several hours or even days depending of the complexity of the case. The result will be data files including similar information as real inspection result files. Using the simulation result files it is possible to create the typical A-, B-, C- and D-scan views for the analysis of the inspection data. Thus it is possible to interpret the results of a virtual inspection in a quite similar way as in the case of a real inspection.

This report gives some general information about ultrasonic part of the Civa simulation program to show some of the possibilities to apply virtual test blocks and inspections. Several simulations (virtual inspections) were run to produce result files which could then be used for analysis trials. According to the analysis results it could clearly be measured that flaw detectability was depending on the size of the flaw and on the other hand also on the probe properties.

2 Brief review of some Civa simulation options

Civa provides a number of component geometries and possibility to define the material properties to produce a realistic component for the simulation. The ultrasonic probe design and characteristics have a wide variety of options. During the simulation the data sampling and probe movement on the component surface can imitate a mechanized inspection.

2.1 Geometry of components

The standard choices for component geometry in Civa (version 9) are: plane, cylinder, cone, sphere, elbow and nozzle. In addition to the standard geometries component geometry can be created using two-dimensional CAD tool (2D CAD) or imported as a 3D CAD model in STEP or IGES format.

However there are some limitations in the use of the various component geometries in different simulation applications. All computations are not necessarily available in all of the geometries and also the scanning movement may be difficult or impossible to accomplish in some geometries using the current program version.

In the following only the simple component geometries are briefly discussed.

2.1.1 Plane

The plane is the simplest component geometry for simulations. The component is rectangular and its dimensions can be freely chosen. A plane component with a scan pattern on its surface is shown in Figure 1. Different flaws can be introduced in the component by defining their shape, size, orientation and location coordinates. The locations of the flaws are defined using component coordinate system.

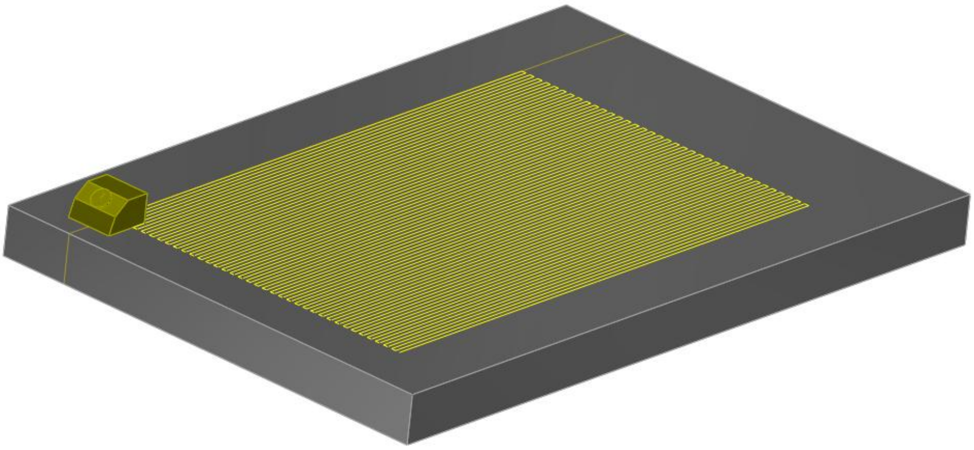

Figure 1. A rectangular component with plane geometry and scan pattern drawn on it.

When the computation is run using scanning shown in Figure 1 the result can be shown as a C-scan view. Anyhow this C-scan shows only the area covered by the scanning and its coordinates refer to the probe positions not to the original component coordinates. The coordinates referring to the actual component coordinates can be read only in the “Cursor” window of the true B-scan view, see Figure 2.

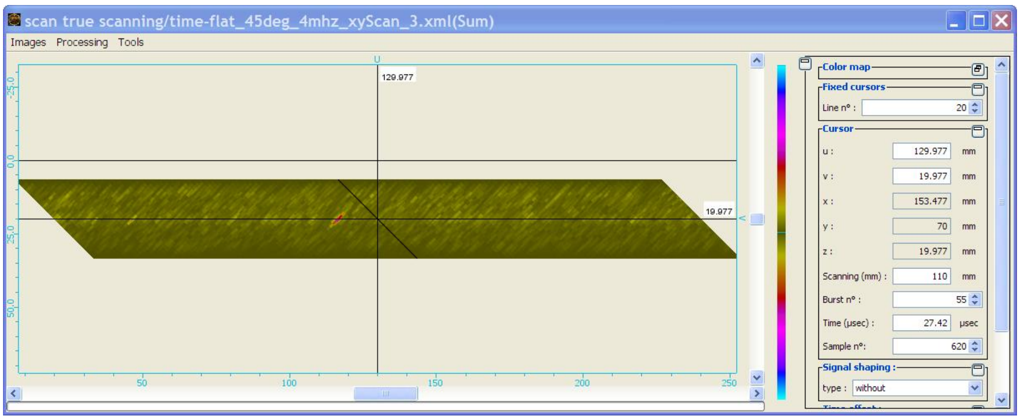

Figure 2. True B -scan view (corrected B -scan) showing the X-, Y- and Z- values for cursor position in the component coordinate system.

2.1.2 Cylinder

Using the component definition option “Cylinder” simple cylindrical or tube formed components can be designed. Different scanning patterns are possible. The flaws can accurately be positioned using component coordinate system. On the other hand the positioning of indications in the data analysis phase is not very convenient and straight forward in the current version (version 9) of the program.

If for example a tube also includes a weld the component should be designed using 2D CAD extension included in the program. Using this option it is possible to define different volumes where material properties may differ. Thus for example the weld and base material can have different attenuation and noise properties. When using this CAD option it is also possible to visualize weld geometry and influence to the location of the origin of the coordinate system, see Figure 3.

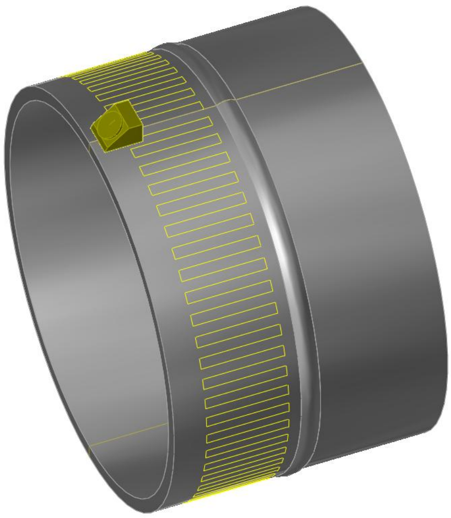

Figure 3. Weld inspection design in 2D CAD module and a scan pattern for the inspection simulation.

2.2 Material properties

The two basic material properties, sound velocity and density, must always be defined because they are taken into account in each computation. In the usual cases these values can be obtained from a list available to Civa program. In addition to these basic parameters also attenuation and structural noise of the material can be included into computation using quite simple definitions.

The attenuation is defined as a frequency depending parameter using either exponential or polynomial attenuation law. The definition is first made in a table format and then the attenuation frequency dependency can be reviewed as a curve, see Figure 4.

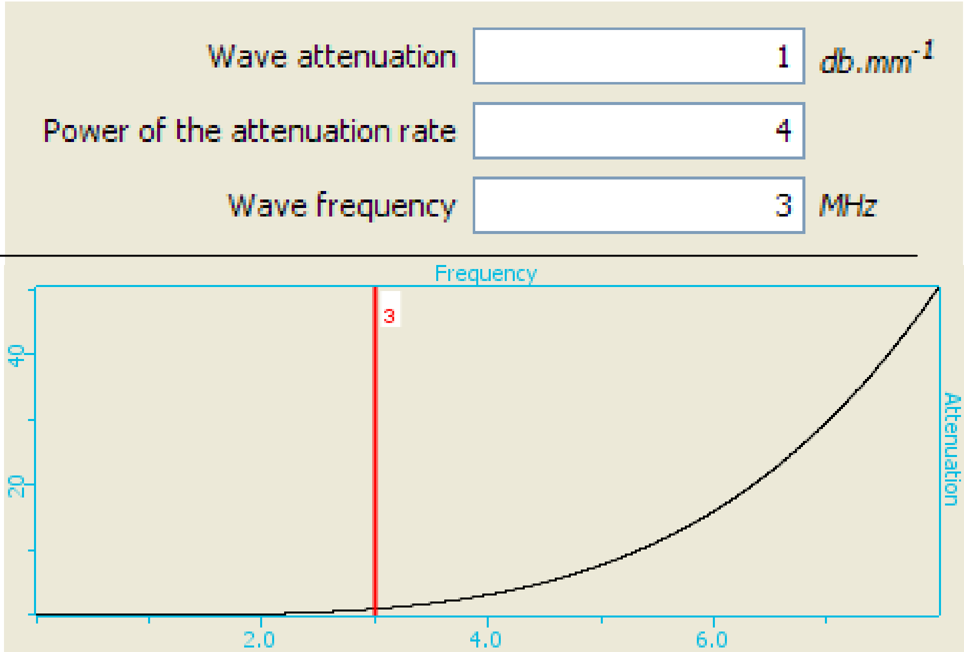

Figure 4. Definition of the attenuation using exponential attenuation law. The table for typing of parameters (top) and the visualization of the frequency dependency (bottom).

The structural noise is modeled using diffracting points randomly positioned in the material. The user has to define the density of these points and also reflectivity amplitude of points. The reflectivity is a zero-mean Gaussian distribution having a standard deviation which is given by the operator.

Civa also provides a possibility to model more complicated material structures e.g. anisotropic welds or multilayer materials. In these cases more material property parameters (for example crystal structure and crystal orientation) must be known and be given for the computation.

2.3 Probe

Civa includes quite extensive possibilities to define different types of probes that are applied in the simulations. The choices include contact, immersion and various phased array probes. The element size and shape as well as the wedge geometry can be exactly defined and also visualized, see Figure 5. The user can set the probe center frequency and bandwidth. There is a wide variety of possibilities concerning phased array probe design and many options are available to create delay laws.

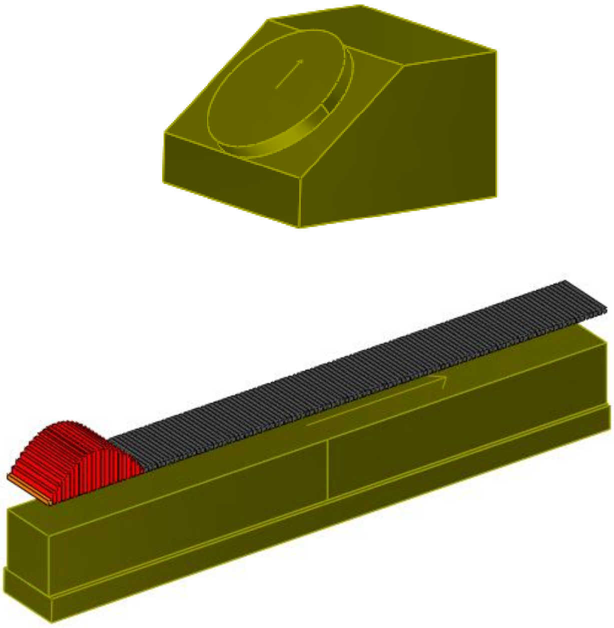

Figure 5. Conventional single crystal probe with an angle wedge and a 128 element phased array probe with a flat wedge designed in Civa. The delay law visualization is presented using red columns.

2.4 Flaws

The typical list of the flaw shapes that can be inserted in the components is: planar rectangular or semi elliptical notch, spherical void, side-drilled hole, flat-bottomed or hemispherical-bottomed hole, planar CAD defect, multifaceted type planar defect, plain cylinder and ellipsoidal inclusion. Some examples of the flaw geometries are shown in Figure 6. The flaw geometries are typically “empty”. The spherical, cylindrical and ellipsoidal shapes can be filled by an isotropic material referring to inclusions.

The dimensions, location and orientation of the flaws can be chosen freely which makes the design and variation of the virtual test pieces very convenient.

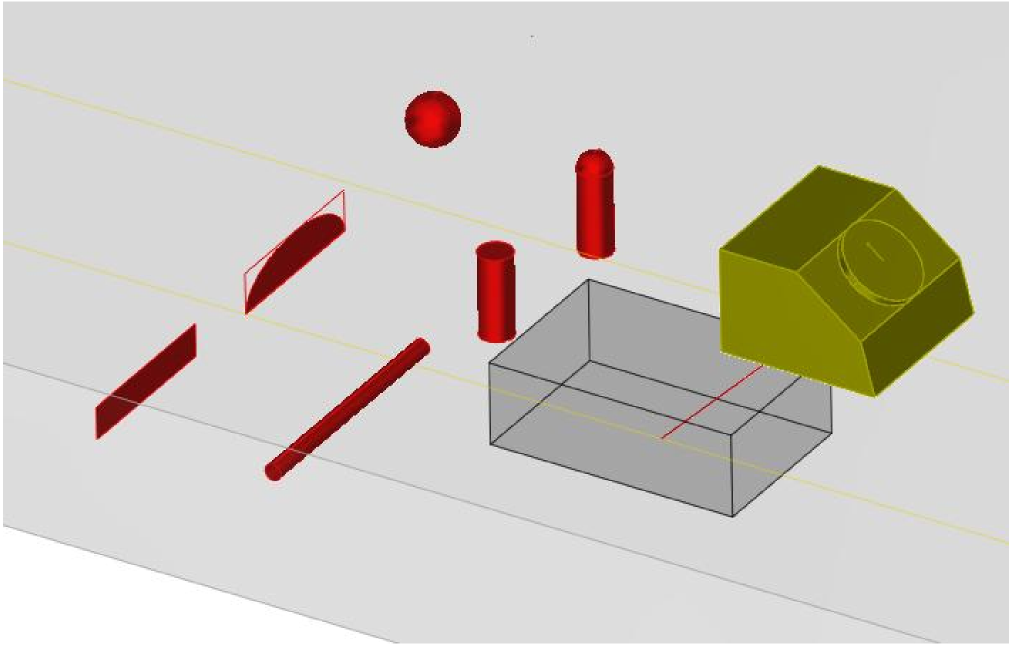

Figure 6. Some examples of flaw shapes in a planar test component.

2.5 Computation

Concerning the computation there are several options to be chosen how the simulation will be performed. For example back wall echoes, corner echoes, surface echoes, mode conversion, shadowing effects etc. can be taken into account if desired. The choice of options available depends to some extent on the applied component geometry and other simulation parameters.

Civa allows the user to specify which flaw scattering model is applied in the computation concerning the ultrasonic beam interaction with flaws. There are three models available and Civa manual states concerning their validity:

- Kirchhoff: Valid for the most of the cases, e.g. specular reflection over planar or volumetric defects. Also corner echo over planar or volumetric defects is computed correctly. There are limitations in computation of tip diffraction signals. Computation of the tip diffraction signals is valid only for the time-of-flight not for the amplitude. The probes (transmitter and receiver) have to be on the “same side” of the defect plane and thus most of the standard cases of TOFD (time-of-flight diffraction) applications are not valid.
- GTD (Geometrical Theory of Diffraction): This interaction model is able to predict echoes diffracted by the edges of planar flaws. Thus it is applicable for TOFD case computations. GTD model is not valid near the specular reflection.
- Born: The flaws filled by an elastic medium and embedded in an other elastic medium can in Civa 9 be modeled using Born approximation.

3 Detectability exercise using a virtual test block

To test the simulation possibilities in assessment of flaw detectablity a virtual test block was designed and then scanned using different probe designs. Finally the data files of inspection simulations were analyzed applying a few procedure-like rules.

3.1 Test block

The virtual test sample applied was a rectangular flat block with dimensions 200 x 300 x 20 mm, see Figure 7. The material of the block was stainless steel. To make the inspection more challenging and realistic some noise and attenuation was defined using the material properties parameters. The noise parameters applied were: density 0.2 pts/mm^3 and amplitude 60 S.I. (in the first simulation 50 S.I). The attenuation was defined according to exponential attenuation law having value of 0.025 dB/mm at 2 MHz and 0.2 dB/mm at 4 MHz for both longitudinal and transversal wave modes.

Several defects were set on the surface opposite to the scanning surface. Some pretest trials were performed varying different defect parameters (height, length, tilt angle and skew angle). Finally it was decided to vary only the height (depth) of the defects to see better the effect of one certain parameter on the detectablility. The shape, orientation and length of the defects were kept same for all defects. The flaws were semi-elliptical notches with length of 10 mm.

Based on the pretest results the defect height between 0.5 - 1.0 mm was seen interesting considering detectability. Thus this range was applied and randomized when choosing the defect heights. When the above presented material and defect parameters were applied it was obvious that some defects could not be distinguished among the noise signals with the probe specifications applied in the pretests. Thus it would depend on the inspection technique and probe characteristics how successful the inspection would be.

The general view of the virtual inspection in the simulation program is shown in Figure 7. The test block can be changed opaque and thus it is possible to hide the defects. However any program user is able to turn the test block transparent and view the defects and also access the defect definition information.

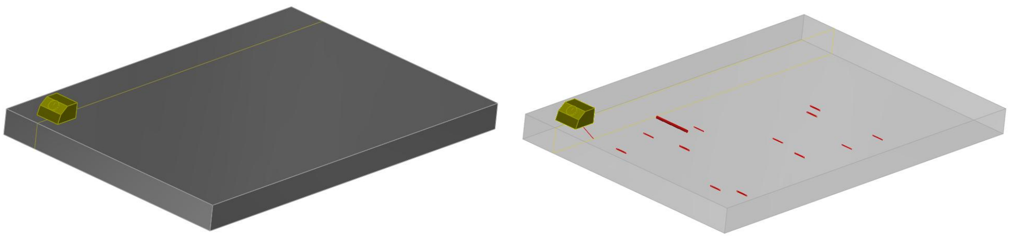

Figure 7. Virtual test block (opaque) and the probe at the scan start position (left). Locations of the defects on the block back surface when the block is made transparent.

An exact top view of the locations of the notches (D2 - D13) and the side-drilled hole (D1) is shown in Figure 8. The positions for the defects were randomized in the area that was chosen to be scanned.

One side drilled hole (∅ 2 mm) was also positioned in the block at the depth of 15 mm for calibration purposes. All the flaw size and positioning information is given in Table 1.

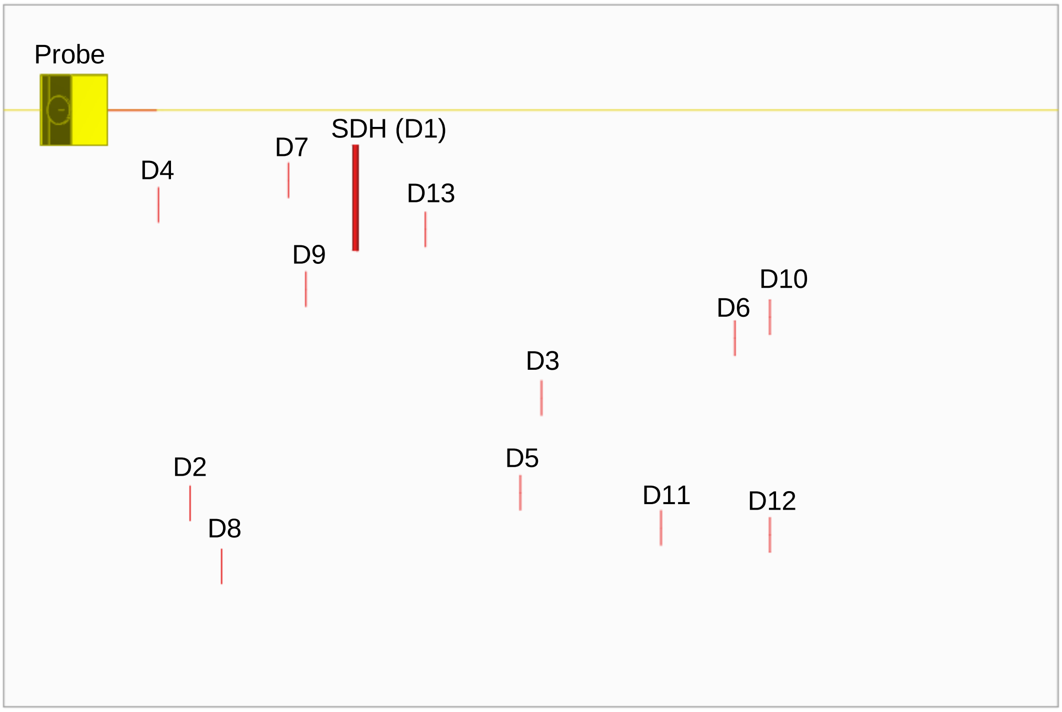

Figure 8. Locations of the semi-elliptical notches (D2 - D12) and side-drilled hole (D1) in the block (top view). Also probe is shown in its scan start position.

Table 1. Flaw dimensions and positions.

ID	Type	Length	Height	X	Y
D1	SDH	30	2	100	55
D2	Semi-ell.	10	0.8	53	142
D3	Semi-ell.	10	0.6	153	112
D4	Semi-ell.	10	0.8	44	57
D5	Semi-ell.	10	0.8	147	139
D6	Semi-ell.	10	0.9	208	95
D7	Semi-ell.	10	0.6	81	50
D8	Semi-ell.	10	0.9	62	160
D9	Semi-ell.	10	1	86	81
D10	Semi-ell.	10	0.9	218	89
D11	Semi-ell.	10	0.5	187	149
D12	Semi-ell.	10	0.5	218	151
D13	Semi-ell.	10	0.5	120	64

3.2 Scanning

Data was “acquired” using a simulation computation. In this simulation the data was “sampled” using 1 mm steps in scan direction and using 2 mm steps in index direction (step between scan lines).

The simulation runs ("scans") were made using several different probe types varying their frequency and crystal size. The applied probes were "created" rather freely and the parameters are not directly equivalent with any existing probe. The applied probe designs in the 12 simulations made are given in Table 2. The purpose was to find out if some clear differences could be seen between the performances of the probes.

Table 2. Probe designs applied in the simulations.

Case ID	Frequency (MHz)	Element shape	Element/ aperture size (mm)	Focus depth (mm)
Simulation 1	4	Circumferential	10	None
Simulation 2	4	Circumferential	10	None
Simulation 3	4	Circumferential	8 mm	None
Simulation 4	4	Phased-array	20x17	20
Simulation 5	4	Circumferential	12	None
Simulation 6	4	Circumferential	6	None
Simulation 7	1	Circumferential	12	None
Simulation 8	2.5	Circumferential	12	None
Simulation 9	1	Rectangular	20x22	None
Simulation 10	2	Rectangular	8x8	None
Simulation 11	4	Rectangular	8x9	None
Simulation 12	2	Rectangular	20x22	None

After simulation computation the result was available as A-, B-, C- and D- scan presentations which are typical presentations of mechanical ultrasonic inspection data.

3.3 Data analysis

The simulation result files are very much similar to those that can be obtained from real ultrasonic inspections thus similar analyzing methods as for the measurement data can be applied. To make the analysis somehow consistent a few principles were decided before starting work forming a short and simple "procedure" including the following issues:

The detection target was set quite strictly:

- flaws are open to the back wall
- flaws are perpendicular to scan axis, skew angle 0°
- flaws are perpendicular to block back wall, tilt angle 0°
- flaw height is 0.5 - 1.0 mm
- flaw length is 10 mm

To identify relevant indication following detection criteria was set:

- signal-to-noise ratio ≥ 6 dB
- indication visible at least in two scan lines

Measurement of indication amplitude and boundaries:

- amplitude measurement in Civa: use A-scan with "envelope".
- indication boundary measurement using - 6 dB drop technique

The analysis was performed by same person who had set up the simulations. All simulations were run as batches and analyses were made separately after considerable time period without checking the real flaw positions at that time. Only when all indications considered being flaws were recorded the findings were compared to the real flaw positions.

The analysis was made using A-, B- and C-scan views. The maximum amplitude value and location coordinates in all three directions were measured for each indications considered relevant. Also the simulation noise level was measured.

4 Results of the simulation trial

In the following two figures (Figure 9 and Figure 10) are shown C-scan views as visual examples of the scan (simulation) results. Figure 9 shows a result where indications from all defects are clearly visible and can be easily distinguished from the material noise. The next figure (Figure 10) presents situation where the noise level is very high compared to the indication signal level and it is very difficult to detect any of the notch indications. Only the echo from the SDH has some higher amplitude compared to the noise level.

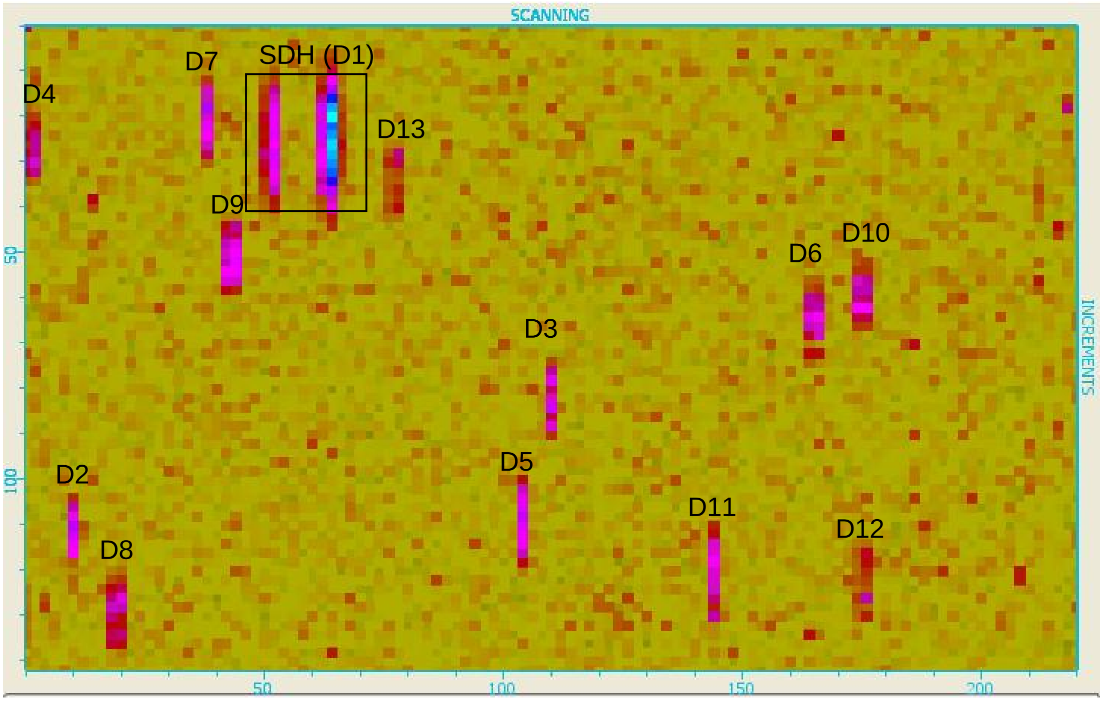

Figure 9. C-scan result when a phased-array probe with focus at the back wall depth was applied in one of the simulations (simulation ID: Sim4).

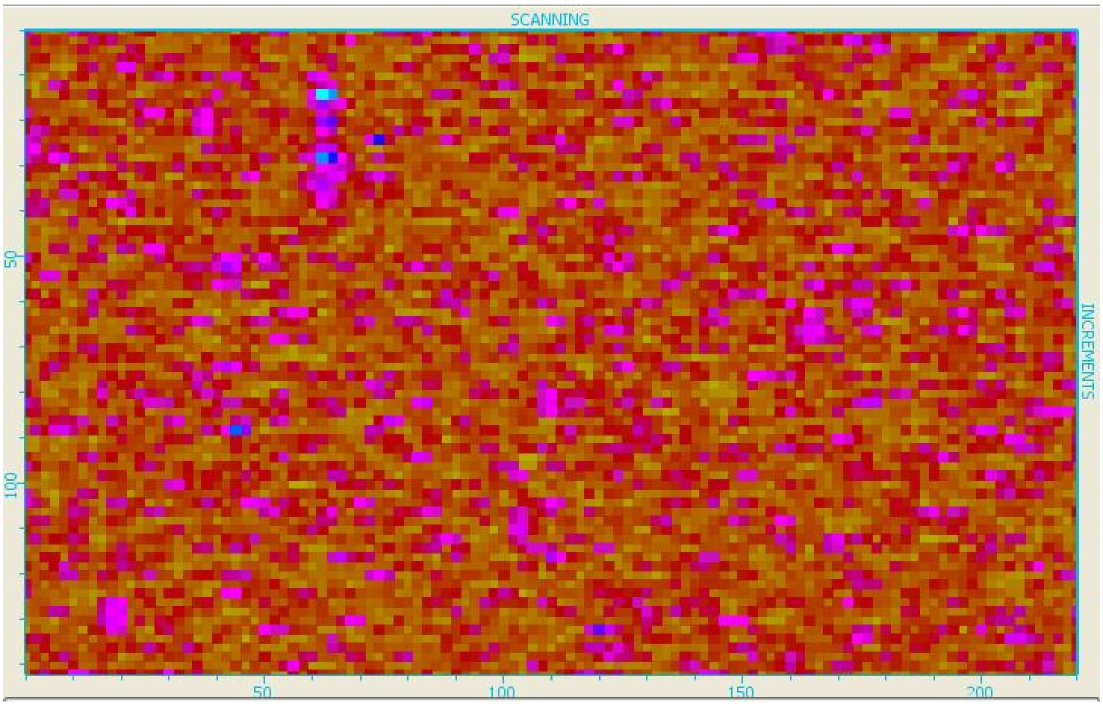

Figure 10. C-scan result when a 4 MHz probe with circumferential ∅ 6 mm crystal was applied in the simulation (simulation ID: Sim6).

Altogether 12 simulations were analyzed. The scan views of these simulations are presented as C-scans in the Appendix 1. The noise level in each simulation was approximated by reducing the amplitude level in analysis phase until only some noise signals were visible. The C-scan views achieved in this way are also presented in Appendix 1. The noise level definition was only an approximation and some variation can be noticed when examining the C-scans where the noise is cut.

The search of indications was based in the first place on the high amplitudes but signal dynamics and repetition in adjacent scan lines were also examined. Thus also many indication signals below the acceptable S/N ratio were identified (breaking the rule that S/N ration should be ≥ 6 dB) and measured. The S/N ratios of all indications that could be detected somehow reasonably are given in Table 3. The high noise level in some simulations caused also recording of two false calls.

Table 3. S/N-ratios of detected indications. Values that are below the acceptable value (6 dB) are indicated using red color.

Simul. ID	Probe characteristics	Defect ID / height (mm)												False calls
		D9	D8	D6	D10	D2	D5	D4	D7	D3	D11	D12	D13	
		1	0.9	0.9	0.9	0.8	0.8	0.8	0.6	0.6	0.5	0.5	0.5	
Sim1	4 MHz, crystal diam. 10 mm	8.5	8.2	8.2	7.4	8	6.5	5.7	5	3.9	5.4		4.2	-
Sim2	4 MHz, crystal diam. 10 mm	7.5	6.8	6.1	6.2	5.4		5.6						1
Sim3	4 MHz, crystal diam. 8 mm	6.1	6.2	5.9	6.5	5.1	5.1							-
Sim4	4 MHz, PA FD = 20 mm	8.2	6.9	7.3	7.7	9.2	8.8	6.4	9.1	8.6	7.4	6.1	5.1	-
Sim5	4 MHz, crystal diam. 12 mm	8.7	7.5	7.1	7.9	5.4	6.6	9.2	3.5	4.7	5.3	5.2		-
Sim6	4 MHz, crystal diam. 6 mm	3.9	2.8	3										-
Sim7	1 MHz, crystal diam. 12 mm	11.6	9.6	9.9	11.1	7.4	8.2	9.3	5					-
Sim8	2.5 MHz, crystal diam. 12 mm	12.1	10.8	10.9	11.2	8.8	9.9	10.6	9.4	7.1	5.6	6.6		-
Sim9	1 MHz, crystal 20 x 22 mm	10.2	9.2	8.8	9.5	7.7	7.9	7.9						-
Sim10	2 MHz, crystal 8 x 9 mm	12	11	11.1	10.8	10.4	10.3	9.3	6	7.7	7.5			-
Sim11	4 MHz, crystal 8 x 9 mm	6.4	5.6	7.4	6	7	5.9	5.4	3.5	4.5	4.4			1
Sim12	2 MHz, crystal 20 x 22 mm	6.7	7.2	7.9	6.9	5.5	6.4	7.5						-

The result concerning detection of the notches is shown below in Table 4. In the column “detection all” the total number of the detected notches is given regardless of the S/N -ratio. According to the “analysis procedure” the S/N -ratio should have been ≥ 6 dB in case of acceptable detection. When taking into account this rule the number of detected defects is considerable lower as it can been seen in the “Detection S/N ≥ 6 dB” column of Table 4.

Table 4. Number of detected flaws in different simulations taking and not taking into account the rule S/N ≥ 6 dB. Also detection rate as percentage is given in both cases. Average of S/N ratios of all detections made is given in the last column. S/N ratio measured from ∅ 2 mm SDH and 1 mm notch is given as a reference.

Simulation ID	Applied probe characteristics	Detection all number	Detecton all (%) percentage	Detection S/N ≥ 6 dB number	Detection S/N ≥ 6 dB percentage	SDH S/N dB	1 mm notch S/N dB	Average S/N dB
Sim1	4 MHz, crystal diam. 10 mm	11	92	6	50	8.2	8.5	6.5
Sim2	4 MHz, crystal diam. 10 mm	6	50	4	33	6.1	7.5	6.3
Sim3	4 MHz, crystal diam. 8 mm	6	50	3	25	7.5	6.1	5.8
Sim4	4 MHz, PA FD = 20 mm	12	100	11	92	12	8.2	7.6
Sim5	4 MHz, crystal diam. 12 mm	11	92	6	50	6.5	8.7	6.5
Sim6	4 MHz, crystal diam. 6 mm	3	25	0	0	6.7	3.9	3.2
Sim7	1 MHz, crystal diam. 12 mm	8	67	7	58	18	11.6	9.0
Sim8	2.5 MHz, crystal diam. 12 mm	11	92	10	83	10	12.1	9.4
Sim9	1 MHz, crystal 20 x 22 mm	7	58	7	58	17.5	10.2	8.7
Sim10	2 MHz, crystal 8 x 9 mm	9	75	9	75	11.2	12	9.6
Sim11	4 MHz, crystal 8 x 9 mm	10	83	4	33	6.6	6.4	5.6
Sim12	2 MHz, crystal 20 x 22 mm	7	58	6	50	14	6.7	6.9

5 Discussion

5.1 Analysis process

The data files produced by simulation can be seen quite realistic from the data analysis point of view. The analysis process of the data in Civa program is similar as the analysis of real data files acquired using ultrasonic equipment. Thus simulations could well be used as training material for data analysis of ultrasonic inspection when Civa is used as the analysis program.

In the simulation the level and location of the noise can be controlled and defined to resemble some known real inspection case. Also the attenuation can be set according to the real situation to make the simulation realistic. These both material parameters can be set by material zone or zones to imitate for example the variation of material properties in base and weld material.

In this simulation exercise the data analysis was made by the “creator” of the virtual test block. Anyway the location of the defects and the depth variation was randomized. Also the simulations were run as batches and finally analyzed after some weeks without checking the defect information. In that sense some level of “blind testing” could be achieved. Also the application of predefined rules in the detection process made the analysis more or less independent of the analyst.

It would be useful to apply real blind analysis in such cases where POD assessments are made using simulation result files. This would require different persons for final defect setup/simulation runs and analysis phase. Also it would be a desired feature of the simulation program if the defect information could be completely hidden from the analyst. So far such feature is not available.

5.2 Detectability

In the simulations only certain narrow defect depth interval from 0.5 mm to 1.0 mm was applied. This defect size range was considered to cause reasonable variation in detectability of the applied notches.

Table below shows how well the notches with different depths were detected both with and without the 6 dB S/N -ratio requirement. It must be noticed that the result is summary achieved using different probe characteristics, some showing very good performance some showing poor performance. In this case one could state that detection of 1 mm notch was reliable using nearly “any probe design”.

Table 5. The detection rate of the notches with different depths.

Notch depth (mm)	1	0.9	0.8	0.6	0.5
Detection possibilities	12	36	36	24	36
Detected all	12	35	31	13	11
Detected with S/N ≥ 6 dB	11	31	22	6	4
Detected all (%)	100	97	86	54	31
Detected with S/N ≥ 6 dB (%)	92	86	61	25	11

Some kind of trial was made to draw probability of detection (POD) curves using the data of Table 5. These curves are shown in Figure 11.

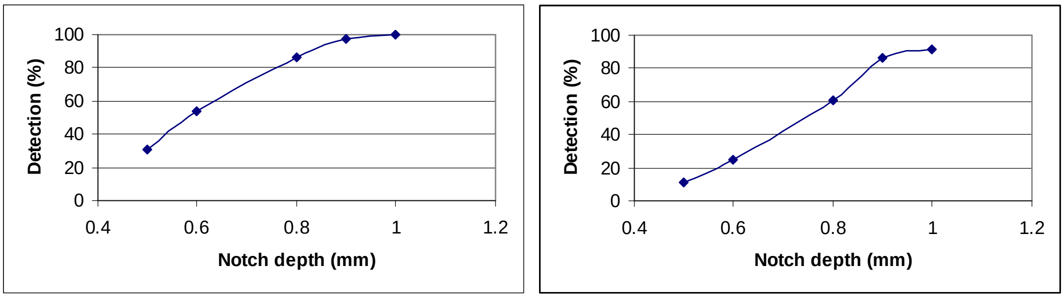

Figure 11. Percentage of detected notches versus notch depth. Left using detection with all S/N -ratios and right taking into account only detection with S/N -ratio ≥ 6 dB.

The two graphics (Figure 12) below are presenting how the defects were detected at different S/N ratio levels. In these graphics the S/N ratio is the average of all hits made with certain probe. In this trial the number of defects is low per each probe arrangement and cannot produce any statistically reliable result. But running simulations repeatedly with same settings more data could be generated to achieve also statistically meaningful results because the noise is randomized in every single simulation.

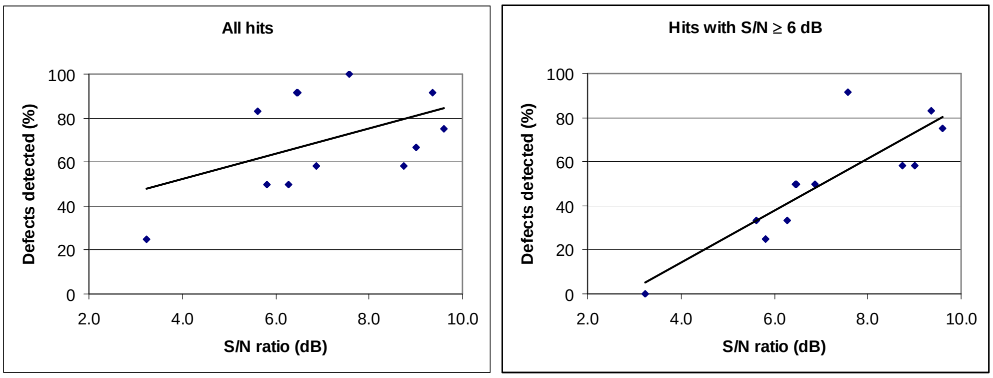

Figure 12. Percentage of detected notches versus S/N ratio. Left using detection with all S/N -ratios and right taking into account only detection with the rule "S/N -ratio ≥ 6 dB".

6 Conclusions

The simulation examples presented in this report show that quite realistic "inspection" data files could be produced using simulation program. By using noise and attenuation controls it is possible to hide the flaws in the virtual test block. Thus the indications arising from the flaw are not obvious and useful challenges can be created for the data analysis.

For imitation of an existing inspection case it would be necessary to match a simulation with a real inspection. This would require measurement of the existing noise level in a representative test block. After that the noise level and appearance should be adjusted and tested through trials in the simulation to find the equivalent level.

The simulation data and analysis result seem to provide material that could be used in POD assessments. It is obvious that the starting point of POD definition should be based on data from real experimental measurements. But because the amount of experimental data is often limited addition of data quantity and extension of parameter limits could be made using simulations.

Some other interesting possibilities to apply virtual test blocks would be personnel training of both on inspection techniques and on data analysis. It could also be possible to organize personnel qualification on data analysis applying data files from simulations.

Concerning serious data generation for POD assessments and personnel qualifications there would be a requirement for blind tests (data analysis). This could be organized quite easily if in the simulation result files the flaw information could be hidden or completely removed.

The advantage of the application of virtual test blocks is production of virtual inspection data at low costs. Even if simulation computations can take hours or days a computer can work by it self after the parameters are set. There is a great freedom and flexibility to change and vary defect and component parameters. The changes of inspection techniques and probe characteristics are also possible very easily.

Appendix 1

C-scan views of the simulations

Left column: full amplitude scale
Right column: only signal above defined noise level visible.

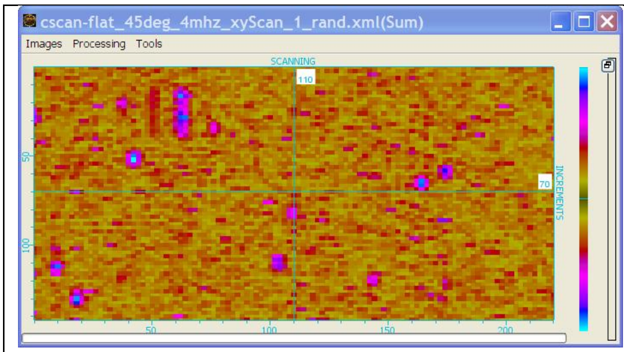

4 MHz, crystal diam. 10 mm (Sim1)with noise Noise amplitude 50 S.I.

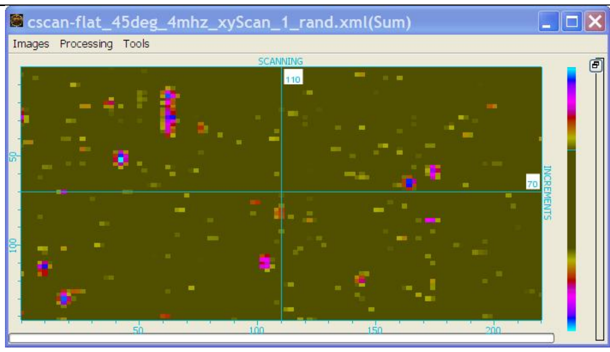

4 MHz, crystal diam. 10 mm (Sim1), noise cut at -8.5 dB

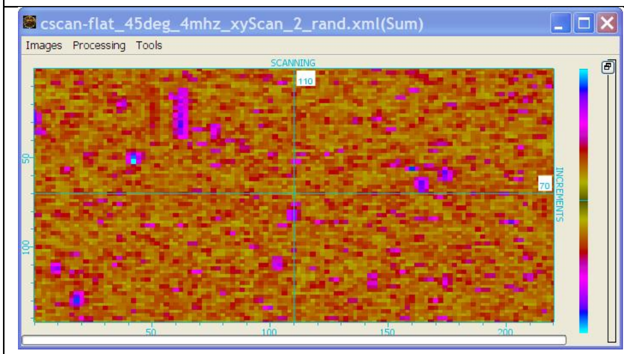

4 MHz, crystal diam. 10 mm (Sim2)with noise Noise amplitude 60 S.I.

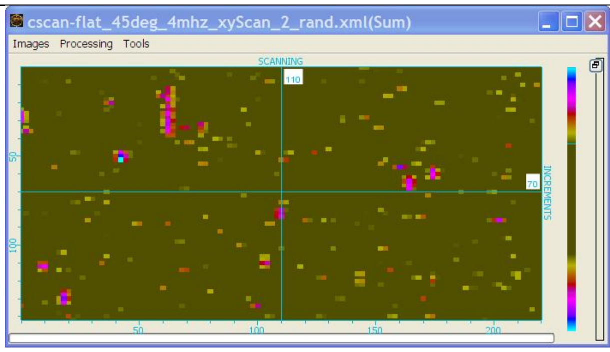

4 MHz, crystal diam. 10 mm (Sim2), noise cut at -7.5 dB

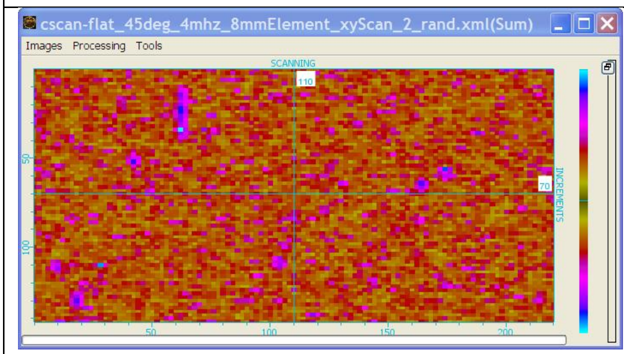

4 MHz, crystal diam. 8 mm (Sim3)with noise

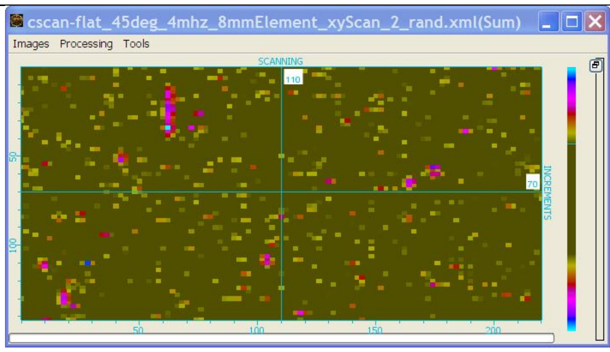

4 MHz, crystal diam. 8 mm (Sim3), noise cut at -7.5 dB

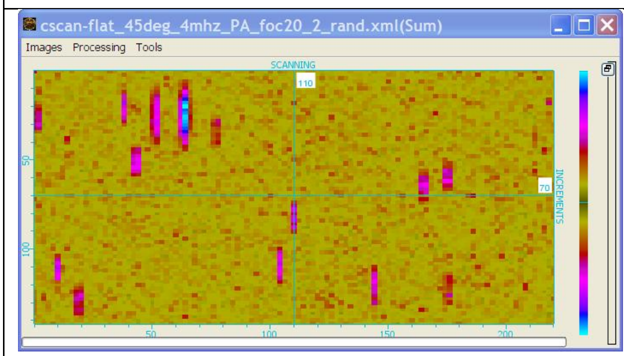

4 MHz, PA, FD=20 mm (Sim4)with noise

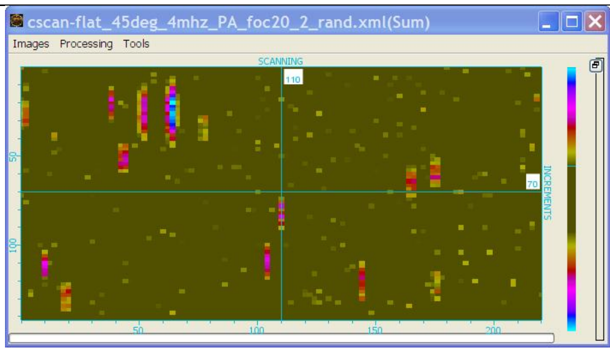

4 MHz, PA, FD=20 mm (Sim4), noise cut at -12 dB

Appendix 1

C-scan views of the simulations

Left column: full amplitude scale
Right column: only signal above defined noise level visible.

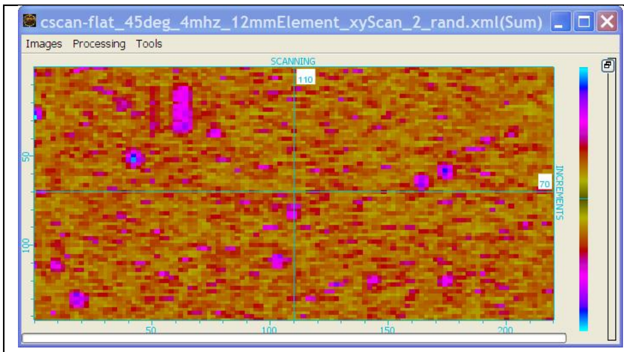

4 MHz, crystal ∅12 mm (Sim5)with noise

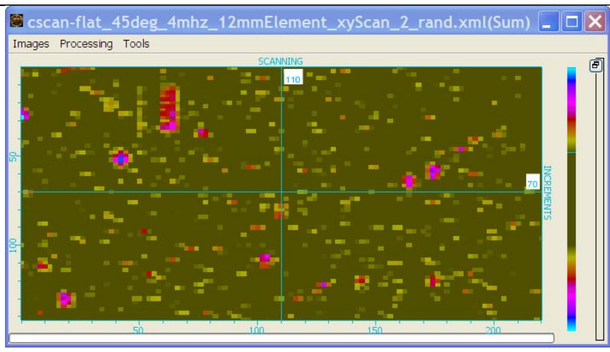

4 MHz, crystal ∅12 mm (Sim5) noise cut at -9 dB

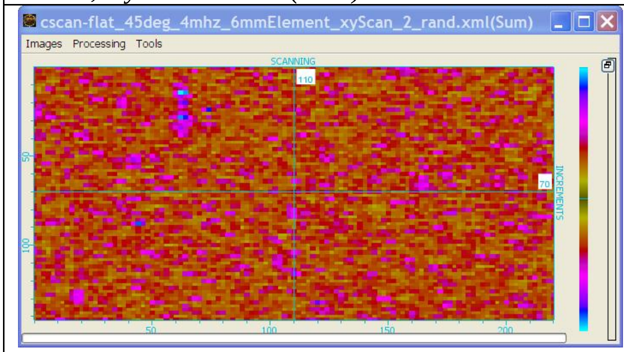

4 MHz, crystal ∅6 mm (Sim6)with noise

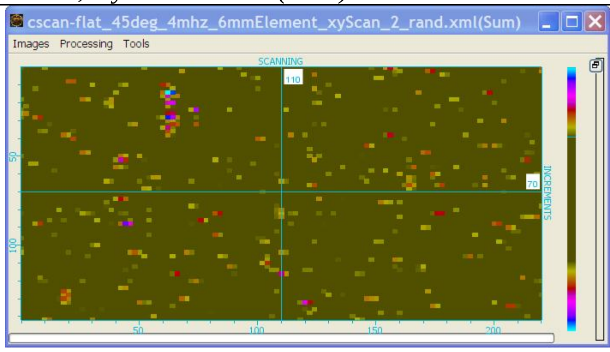

4 MHz, crystal ∅6 mm (Sim6) noise cut at -6.5 dB

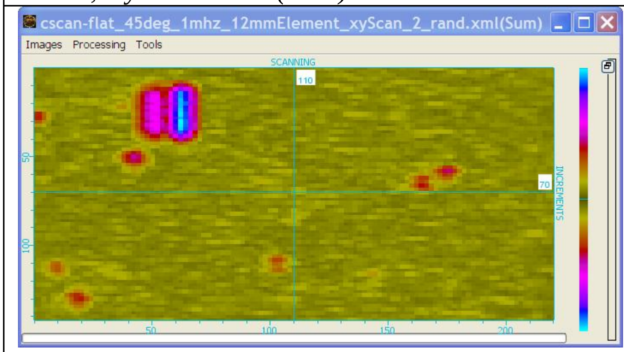

1 MHz, crystal ∅12 mm (Sim7)with noise

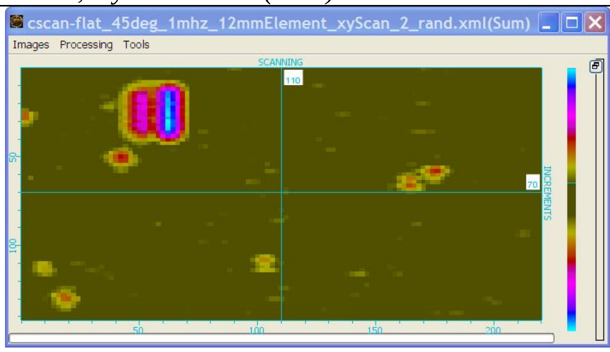

1 MHz, crystal ∅12 mm (Sim7) noise cut at -18 dB

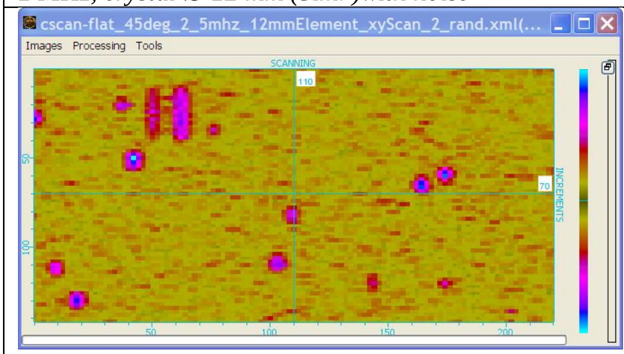

2.5 MHz, crystal ∅12 mm (Sim8)with noise

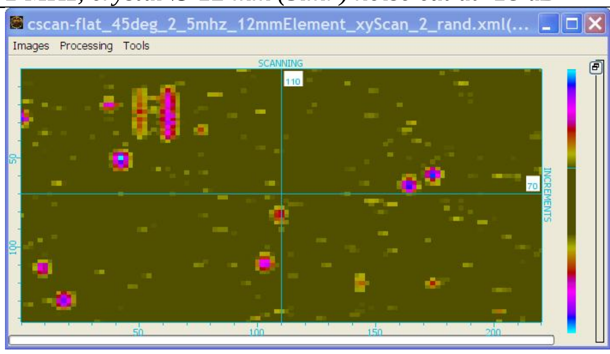

2.5 MHz, crystal ∅12 mm (Sim8) noise cut at -12 dB

Appendix 1

C-scan views of the simulations

Left column: full amplitude scale
Right column: only signal above defined noise level visible.

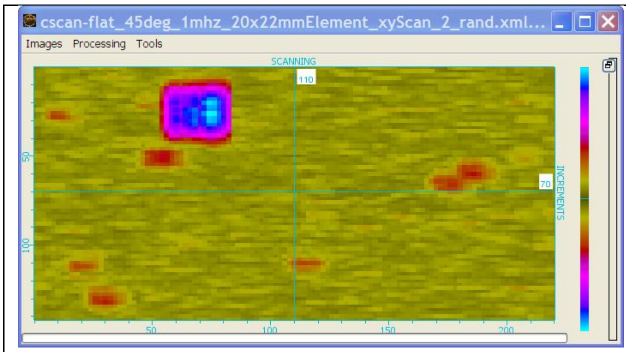

1 MHz, crystal 20 x 22 mm (Sim9)with noise

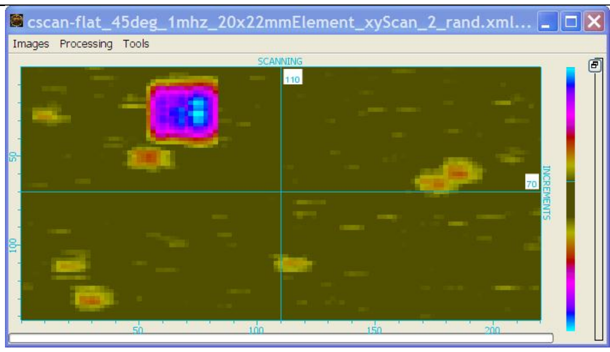

1 MHz, crystal 20 x 22 mm (Sim9) noise cut at -17.5 dB

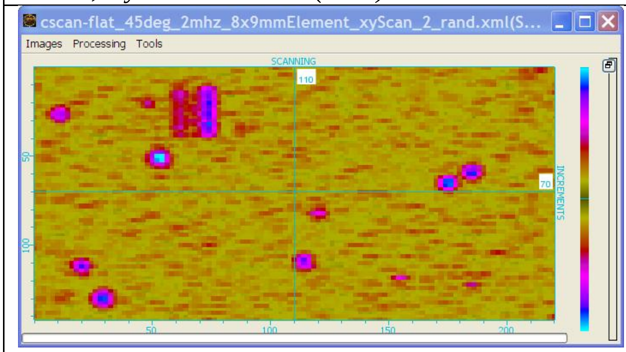

2 MHz, crystal 8 x 9 mm (Sim10)with noise

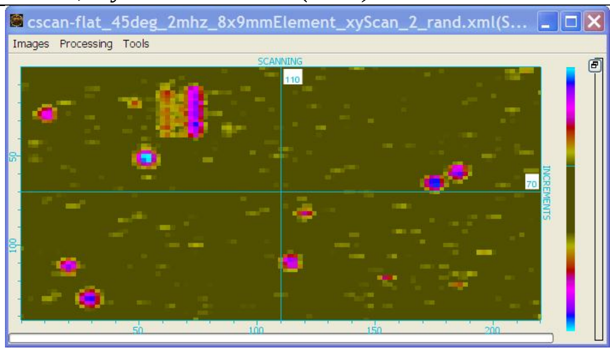

2 MHz, crystal 8 x 9 mm (Sim10) noise cut at -12 dB

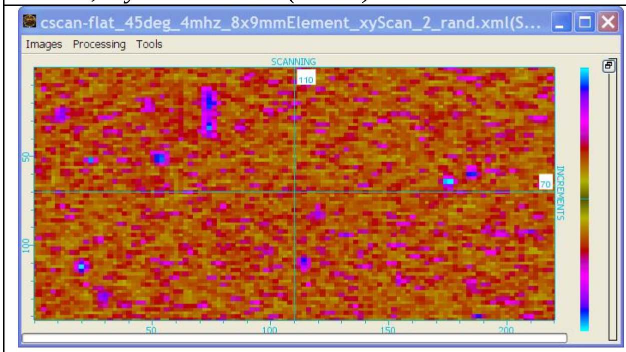

4 MHz, crystal 8 x 9 mm (Sim11)with noise

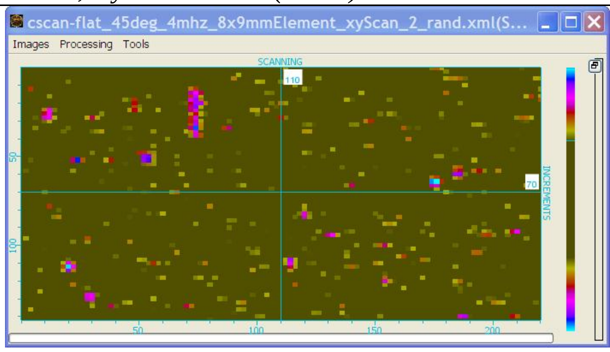

4 MHz, crystal 8 x 9 mm (Sim11) noise cut at -7 dB

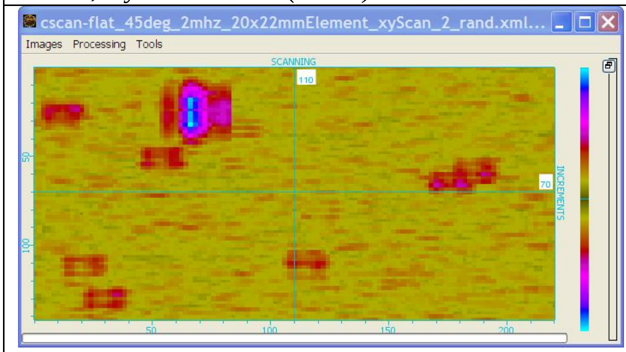

2 MHz, crystal 20 x 22 mm (Sim12)with noise

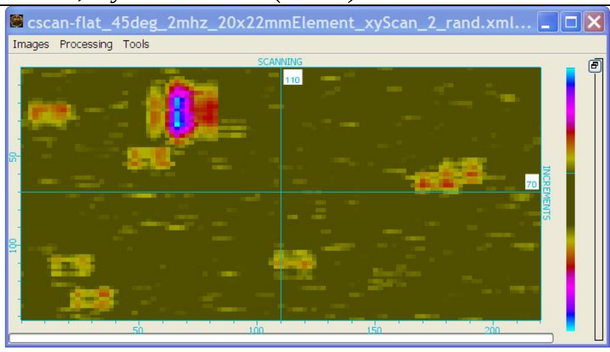

2 MHz, crystal 20 x 22 mm (Sim12) noise cut at -14 dB